Alterations in Cardiovascular and Cerebral Pulse Wave Velocity in 5XFAD Murine Model of Alzheimer's Disease

Authors and Affiliations:

Andrea G. Marshall[1,*], Kit Neikirk[1,*], Taylor Barongan[1], Bryanna Shao[1], Amber Crabtree[1], Dominique Stephens[1,2], Zer Vue[1], Heather K. Beasley[1], Edgar Garza-Lopez[3], Estevão Scudese[2], Steven Damo[2], Jose A. Gomez[5], George E Taffet[6], Antentor O. Hinton, Jr[1,#], Anilkumar K. Reddy[6,#]

[1] Department of Molecular Physiology and Biophysics, Vanderbilt University, Nashville, TN, 37232, USA.
[2] Department of Life and Physical Sciences, Fisk University, Nashville, TN, 37232, USA.
[3] Laboratory of Biosciences of Human Motricity (LABIMH) of the Federal University of State of Rio de Janeiro (UNIRIO), Rio de Janeiro, Brazil; Sport Sciences and Exercise Laboratory (LaCEE), Catholic University of Petrópolis (UCP), Brazil
[4] Department of Internal Medicine, University of Iowa, Iowa City, IA, 52242, USA.
[5] Department of Medicine, Vanderbilt University Medical Center, Nashville, TN, 37232, USA
[6] Department of Medicine, Baylor College of Medicine, One Baylor Plaza, Houston, TX 77030, USA.

Running Title:

Corresponding Authors

Anilkumar K. Reddy, Ph.D.
Department of Medicine
Baylor College of Medicine
One Baylor Plaza, MS: BCM285
Houston, TX 77030, USA.
Ph: 713-798-6831
Email: areddy@bcm.edu

Antentor O. Hinton, Jr, Ph.D.
Department of Molecular Physiology and Biophysics
Vanderbilt School of Medicine Basic Sciences
The Vanderbilt Diabetes Research and Training Center
750 Robinson Research Building
2200 Pierce Ave
Nashville, TN 37232-0615
319-383-3095 (cell)
antentor.o.hinton.jr@Vanderbilt.Edu

Abstract:
Alzheimer's Disease (AD) is a global health issue, affecting over 6 million in the United States, with that number expected to increase as the aging population grows. As a neurodegenerative disorder that affects memory and cognitive functions, it is well established that AD is associated with cardiovascular risk factors beyond only cerebral decline. Using novel techniques of cerebral and cardiovascular-related pulse wave velocity parameters in 5x transgenic mice with AD, we examined the sex-dependent differences in AD. Specifically, we measured cardiovascular pulse wave velocity parameters, a marker of arterial stiffness and cardiovascular risk, and cerebral pulse wave velocity, a novel technique to measure cerebral blood flow. Our results showed that 5x transgenic mice had reduced ejection time, pulse pressure, and Tei index, with slight sex-dependent differences. However, many other cerebral blood flow and pulse wave velocity measurements indicated diet did not significantly alter cardiovascular risk. Beyond this, sex-dependent differences highlight slight cardio-protective effects in female mice in control AD mice; however, these sex-dependent differences must be explored further. Together, these highlighted increased arterial stiffness and cardiovascular Future research may explore how the effects of modifying factors including age, chronic diet, and acute stress, which may further affect the stress-dependent progression of cardiovascular risk in AD.

Keywords: Alzheimer's Disease, 5xFAD, Pulse Wave Velocity, Cardiovascular Disease

Introduction:

Alzheimer's disease (AD) is a progressive neurodegenerative disorder that affects millions of people worldwide and causes deficits in quality of life and daily living marked by a decline of memory and cognitive functions (Wong, 2020). AD remains a critical disease to investigate as no treatments yet exist for it while the estimated yearly burden on it amounts to $305 billion, an amount that is expected only to grow with the aging population (Wong, 2020). A hallmark feature of AD is the accumulation of aggregated amyloid beta (Aβ) protein in the brain, which ultimately leads to synaptic dysfunction, neuronal loss, and cognitive impairment (Scheltens et al., 2016). In addition to genetic factors, lifestyle and environmental factors such as stress and diet have been implicated in the development and progression of AD (Silva et al., 2019). Beyond dementia, AD also impacts cardiovascular function, as the amyloid beta plaques also accumulate in the heart (DeCarli, 2021). A key risk factor of AD is hypertension, and it has been hypothesized that neuroinflammatory effects link these pathologies (Bajwa and Klegeris, 2022). However, the full extent of the mechanisms which link AD and cardiovascular disease remains poorly understood. Here, we sought to expand the understanding of how AD alters cardiovascular and cerebral blood flow in conditions of chronic diet changes or acute stress.

AD is well understood to cause neuropsychologic decline but is also understood to affect cardiovascular dynamics. AD importantly is shown to potentially be associated with HTN through the formation of neuritic plaques in HTN, potentially through limiting cerebral blood flow (Eglit et al., 2020). In human populations, even when correcting for risk factors such as age, HTN reduction is correlated with increased cognitive ability retention, causing blood pressure treatment to arise as a potential mechanism to treat AD (DeCarli, 2021). This blood pressure linkage to AD is especially pronounced when it comes to the systolic pressure (Lennon et al., 2019). However, a past review on the matter shows the issue to be far more complicated, as many previous studies are not using standardized HTN measurements and there may be age-

dependent and ethnicity-dependent influences of HTN on AD development (Hughes et al., 2015). Together, this underscores the need to better understand hemodynamics in AD.

Hemodynamics including pulse wave velocity (PWV) are important methods to study cardiovascular function and aortic stiffness. Even when adjusting for factors including age, race, and disease states, registry studies indicate PWV remains a strong predictor of overall mortality in human populations (Heffernan et al., 2020). Past studies looking at echocardiographic parameters in humans with AD showed that diastolic function was more heavily impacted in AD pathology, marked by increased arterial stiffness, increased atrial conduction times, reduced blood flow, and altered mitral valve velocities (Çalık et al., 2014). Carotid–femoral pulse wave velocity increased aortic stiffness has also been linked as an independent predictor of cognitive impairment for both dementia and AD (Pase et al., 2016). Another longitudinal study across over 1700 participants found that arterial stiffness and alterations in pulse pressure are antecedents for cognitive decline (Waldstein et al., 2008). PVW can further be used to distinguish vascular dementia and AD, with the former often expressing increased vascular stiffness relative to AD (Rabkin and Jarvie, 2011). Past studies have also highlighted the importance of looking at both PWV as well as brain blood, through MRI, with hypertensive symptoms altering heart and brain structure (Burke and Hughes, 2021). Yet there remains controversy, as some studies have found no correlation between carotid–femoral PWV and AD (Nilsson et al., 2017) and human models remain limited to non-invasive techniques.

Our aim was to look at AD cardiovascular-related parameters in 5x transgenic (5XFAD) mice, mice that have 5 AD-linked mutations. The 5XFAD mouse model expresses human amyloid precursor protein (APP) and presenilin 1 (PS1) mutations, leading to the rapid accumulation of Aβ and the development of AD-like pathology (Oblak et al., 2021). This model also bears numerous similarities to human models including Aβ-butyrylcholinesterase association and hallmarks of progressive loss of cognitive function concomitant with reduced synaptic markers (DeBay et al., 2022). Due to apoptotic neuron loss, 5XFAD mice display memory deficits by 4 months of age (Eimer and Vassar, 2013). This mouse model has been widely used to study the mechanisms underlying AD and to test potential therapeutic interventions. Past studies using 3x transgenic mice models highlight that with induced hypertension, mice had faster development of AD marked by upticks in Aβ, amyloid plaque load, and phosphorylated tau (Shih et al., 2018). This validates that transgenic mice models retain the relationship between cerebrovascular and cardiovascular dysfunction that has been observed in AD.

Our study is further unique in that we present a technique to measure cerebral pulse wave velocity in 5XFAD. The relationship between PWV and AD pathology in 5XFAD models remains unclear, especially as it comes to cerebral pulse wave velocity (cPWV), a hemodynamic parameter that has been increasingly recognized as an important predictor of cerebrovascular disease. While aortic stiffness can serve as a predictor for strokes, it is limited in detection of minor changes which precede cerebrovascular changes such as microbleeds (Henskens et al., 2008). Similar to its aortic counterpart, cPWV measures the speed at which arterial pressure or velocity waves propagate through the cerebral arteries. Measuring cerebral impedance is a novel measure of the comprehensive characterization of cerebral blood vessels, which is highly relevant as the brain is a highly vascularized organ that requires a constant supply of oxygen and nutrients, with disruptions in blood flow being linked to cognitive impairment. In AD, this

remains highly relevant as it may relate to Aβ clearance (Hughes et al., 2015). A recent clinical trial protocol has proposed utilizing Carotid-Cerebral Pulse Wave Velocity as a mechanism to better understand acute ischemic strokes (Zeng et al., 2019). Here, we use pulsed Doppler ultrasound to simultaneously measure the arrival of the velocity wave at two different arterial sites, one at aortic arch and another at mid-cerebral artery, and measure the physical distance between the two sites to estimate cPWV . In this context, understanding the relationship between cPWV and cerebral impedance is crucial for improving our understanding of the pathophysiology of AD.

Of note and novel to this study, we also utilized cerebral pulse wave velocity. This technique, which to our knowledge has not been published before, utilizes measurements of flow velocity in cerebral circulation which, alongside standard measurement aortic arch velocity, allows for blood flow across different systems to be measured (Table 1). Past theoretical frameworks indicate that both arterial pressure, peripheral resistance, and cerebral blood flow play roles in cerebrovascular diseases and Aβ plaques, yet the full extent of hemodynamic changes in 5XFAD models up to this point have remained unclear (Hughes et al., 2015). Additionally, while it is clear that females are more likely to get AD in humans, there remains a gap in the literature in understanding sex-dependent differences in cerebral hemodynamics in 5XFAD models (DeBay et al., 2022). Our findings provide important insights into the relationship PWV and AD pathology, as well as potential novel mechanisms of protection. By understanding how these factors interact to influence arterial stiffness and cognitive function, we may be able to identify new therapeutic targets for the treatment and prevention of AD.

Results:

To begin with, 5 male and female control aged-matched littermates and 9 female and 10 male 5x transgenic mice had their general parameters considered. Body weight and aortic cross-sectional area increased in both males and females (Figures 1A-B), while heart rate (HR) was inversely decreased in 5XFAD mice (Figures 1C). We determined the impact of 5x transgenic on cardiac systolic function and found no notable changes in peak aortic velocity and mean aortic velocity, while aortic ejection time (ET) was impaired (Figure 1D-F). While females have heightened alterations in ET and HR, males inversely showed a larger change in body weight and aortic cross-sectional area in a 5XFAD model compared to females.

The carotid artery peak, minimum, and average velocity showed no significant changes (Figure 2A-C). Similarly, the pulsatility index (PI) and resistivity index (RI), two measurements of velocity to serve as indicators of vascular resistance, showed no significant changes in comparing control and 5XFAD mice in either sex (Figure 2D-E).

Systolic blood pressure (SBP), diastolic blood pressure (DBP), and mean blood pressure (MBP) did not show statistically significant changes across either sex (Figures 3A-C). However, pulse pressure (PP = SBP-DBP) and rate pressure product (RPP = SBP * HR) both decreased significantly in 5XFAD mice compared to the control mice (Figures 3D–F). This was slightly more significant in females, which may be partially explained by the relatively heightened HR in 5XFAD females.

While LV afterload was evaluated using aortic impedance, neither males nor females showed significant differences in the two groups' impedance parameters, Zp, Z1, Zc, or PWVz, although males show a slight but non-significant decrease (Figure 4A-D). When performing the cerebral counterpart to this measurement, we noticed in all measurements females exhibited more variability but only cerebral Zp in females was statistically increased in 5XFAD compared to control mice (Figure 5A-D).

While end-systolic pressure, arterial elastance (Ea), stroke distance, and stroke work exhibited slight differences in comparing control and 5XFAD mice, none of these proved to be statistically significant (Figure 6A-D).

For both male and females, while mitral peak early velocity (E) was slightly increased in 5XFAD mice this was not significant. However, both 5XFAD males and females had significant decreases in both isovolumetric relaxation (IVRT) and contraction time (IVCT), which concomitantly reduced myocardial performance index (MPI, also known as Tei Index). This decrease was slightly larger in female sample mice.

Discussion:

5XFAD mice are important new experimental models for the study of Alzheimer's Disease (Oblak et al., 2021), but such models have limited research evaluating their *in situ* global cardiovascular function. Beyond using noninvasive measurements of Doppler mitral inflow and aortic flow velocity, invasive measurements of aortic and LV pressure, and the calculated aortic impedance, we also evaluated cerebral impedance. This allowed us to consider differed cerebral, cardiac, and aortic hemodynamics in 5XFAD male and female mice compared to their age-matched littermates. The baseline parameters of body weight, aortic cross-sectional area, and heart rate of 5XFAD mice were not significantly different from control mice (Figure 1), indicating that overall cardiac health is affected in mice with AD.

<u>Cardiac systolic and diastolic function</u>

We found that aortic ejection times were significantly reduced in the 5XFAD mice (Figure 1F). Of relevance, reduced left ventricle ejection time is commonly reduced in heart failure with reduced ejection fraction, serving as a negative factor that concomitantly occurs with impaired ejection fraction and stroke volume (Alhakak et al., 2021). In contrast, longer aortic ejection time can result in reduced blood pressures (Obata et al., 2017), although we did not see significant changes in blood pressure. Given we noted a sex-dependent difference in ejection time, this may aid to explain the greater vulnerability of females with AD to cardiovascular diseases. Past studies have shown that β-amyloid deposition typically increased alongside blood pressure in human models (Hughes et al., 2015), so future studies may aid to understand if, in the 5XFAD model which shows no change in overall blood pressure, there are changes in β-amyloid deposition with age.

<u>Aortic and left ventricular pressure</u>

Carotid changes were not noted (Figure 2) and 5XFAD mice also had non-statistically significant changes in diastolic, systolic, and mean pressures compared to control mice (Figure 3). However, pulse pressure was significantly decreased in both models, well below 25% of the value of

systolic pressure, which typically occurs with dysfunction, indicating aortic stenosis, cardiac tamponade, aortic stenosis, or with blood loss (Homan et al., 2018). This effect was especially heightened in females, again pointing towards slight sex-dependent differences. Inversely, human longitudinal studies indicate that increased pulse pressure serves as a marker of impaired cognitive measures and memory (Waldstein et al., 2008). However, a previous study found that reduced pulse pressure occurred alongside impaired cerebral blood flow in AD (Roher et al., 2012). This suggests that 5XFAD models may change across the aging process or that pulse pressure has a more complex relationship in AD. Oxygen consumption is also likely impaired as the rate pressure product (RPP = SBP × heart rate) was reduced in 5XFAD mice.

Aortic and Cerebral impedance

When evaluating the aortic peripheral vascular resistance (Zp,), strength of wave reflections from the periphery (Z1), characteristic impedance (Zc,), and pulse wave velocity (PWV) we did not note a significant difference in 5XFAD mice compared to their control counterpart (Figure 4). Akin to our previous findings (Marshall et al., 2022), it would be expected that pulse pressure and ejection time would concomitantly change with Zc & PWVZ as aortic stiffness index should correlate between these measures, yet we did not observe this. Furthermore, past studies implicated increased arterial stiffness to negative cerebral outcomes in a linear fashion with age (Palta et al., 2019), so it was expected that this increased stiffness would be reflected in these measurements.

Notably, we did see that only females displayed increased cerebral impedance Zp (Figure 5A). This can imply that neurovascular coupling or conduction of electrical signals within the brain may be uniquely impacted in females with AD. This parallels prior results which show that cerebral perfusion, as measured by neuroimaging with single photon emission computed tomography, is unchanged in 5XFAD when compared with the control (DeBay et al., 2022). However, this study (DeBay et al., 2022) aggregated male and female data, suggesting that it is possible a significant difference may only be observed in females. Interestingly, one past study suggested that cerebral blood flow is increased in AD risk states, suggesting a complex relationship between cPWV and AD (Fleisher et al., 2009).

Ventricular-vascular coupling

Ventricular-vascular coupling (VVC) was also examined in 5XFAD mice, which showed no significant changes in stroke work, distance, or other modifiers, indicating potentially largely unchanged global cardiovascular efficiency (Figure 6).

Doppler-Derived Measurements

Isovolumic relaxation time and isovolumic contraction time represent indexes of LV relaxation and contraction times, respectively. Interestingly, past studies show increased IVRT in patients with pulmonary hypertension (Dambrauskaite et al., 2005). Another large population-based study found that even when adjusted for other factors, increases in IVCT were corollary with the occurrence of heart failure (Alhakak et al., 2020). Decreases in IVCT were also noted to occur alongside losses of ejection times and serve as independent predictors for exercise capacity in heart failure (Cho et al., 2010). IVCT and IVRT are both associated with LV ejection time, so

the myocardial performance index (Tei Index) provides an overall systolic and diastolic performance not dependent on ventricular geometry (Liu et al., 2017). Both 5XFAD genders show a decreased Tei Index compared to control littermates, indicating greater cardiac function and reduced risk of HF (Carluccio et al., 2012). Since males show a slightly lower Tei Index than females, this suggests that this cardioprotective effect may be stronger in males. Notably, one past study found that cathepsin D content, which is associated with cardiovascular disease and AD, Tei index is correlated with protein levels, suggesting the changes we observe here may be independent of this protein (Liu et al., 2017). Another study found that isovolumetric relaxation times were increased in AD groups (Çalık et al., 2014). Similarly, an echocardiographic on AD patients showed an increased Tei index compared to age-matched controls (Belohlavek et al., 2009); however, both studies were on an older age cohort suggesting that the cardioprotective effects may diminish across aging.

Future Directions

The findings of this study have important implications for our understanding of measurements of hemodynamic parameters during AD pathology. By better knowing how arterial stiffness changes in 5XFAD models, therapeutic techniques can better be created to target these specific aspects, such as through neuroendocrine therapies (Hughes et al., 2015). For example, tetrandrine-treated 5XFAD mice have been shown to have ameliorated AD through reduced Aβ plaque formation, but it is unclear if new therapies such as these affect hemodynamics (Ren et al., 2021). Other potential therapeutic targets include mitochondria, as mitochondria arise as a potential mechanism to restore against HTN-induced progression of AD. Mitochondrial complex I inhibition results in the lowering of amyloid-ß levels, suggesting modulation of mitochondrial metabolism may modulate AD progression (Zhang et al., 2015). Beyond this, previous reviews have summarized drugs that may increase cerebral perfusion (de la Torre, 2016), but our results indicate that in males at least, cPWV may not be heavily affected in 5XFAD mice.

Future studies can better elucidate vascular cognitive impairment by examining other murine models for dementia to better understand if aspects of 5XFAD mice may present differential hemodynamics (Bink et al., 2013). In the future, cPWV may also aid in the early detection and monitoring of other neurological disorders. While arterial PWV may serve as a mechanism to explore cerebral perfusion, cerebral microbleeds have arisen as markers that are important to study in AD (Hughes et al., 2015). Other studies have also shown that glutamate chemical exchange saturation transfer has been observed to concomitantly decrease with cerebral blood flow in 5XFAD mice, suggesting other novel imaging techniques that can potentially be used alongside cPWV (Igarashi et al., 2020). Another promising technique is 4D flow MRI, which has been used to show increased transcranial PWV in AD (Rivera-Rivera et al., 2021). Therefore, further studies are needed to elucidate the mechanisms underlying how cPWV and other innovative techniques may explore AD in 5XFAD and other models.

Future studies may look at the compounding effects of other experimental changes, such as chronic diet changes, induced hypertension, and acute stress, as the effectors which may more heavily affect the aortic and cerebral PWV of 5XFAD mice than their control counterparts. Additionally, we did not measure other factors that may influence hemodynamic parameters, such as exercise (Tarumi and Zhang, 2014), which could be an important confounding variable.

Furthermore, there is an unmet need of understanding how aortic and cerebral PWV changes across the aging process for 5XFAD. Aging is especially important to study in the context of 5XFAD as they present a truncated development of AD pathology compared to human counterparts, marked by lower levels of Aβ with isomerized D7 and non-linear Aβ accumulation, indicating that aging can uniquely affect 5XFAD mice (Bugrova et al., 2022). Furthermore, past studies have shown that while changes in pulse pulsatility, which we observed, are more common in younger individuals, stiffness is more likely to arise in older AD patients, which may aid to explain why we did not observe as significant changes in our study (McEniery et al., 2005; Palta et al., 2019).

Conclusion:

In conclusion, our study showed no significant changes in most of the hemodynamic parameters examined, with the most pertinent changes observed in ejection time, pulse pressure, IVCT, IVRT, and cerebral impedance Zp, which displayed slight sex-dependent differences. These findings suggest that the relationship between PWV and AD pathology in animal models may be more complex than previously thought and highlight the importance of studying multiple hemodynamic parameters in the context of AD. Females may be more vulnerable to AD partially due to increased cerebral impedance Zp. Ejection time and pulse pressure in 5XFAD animals suggest deteriorating effects, while Doppler-derived measurements conversely suggest potential cardiovascular protective effects. Further studies are needed to elucidate the mechanisms underlying these findings and their implications for the development and progression of AD.

Limitations:

There are several limitations to this study that must be considered when interpreting the results. While 5XFAD mice serve as a strong model for human AD that has been used in the past, it lacks neurofibrillary tangles which human models would otherwise have (Oakley et al., 2006; Oblak et al., 2021). This and other differences in 5XFAD models make it unclear whether our findings can be extrapolated to humans. Another limitation of our study is that we did not measure Aβ deposition levels, which may be correlated with PWV (Hughes et al., 2013), or other molecular markers of AD pathology. Therefore, it is possible that our findings do not fully capture the complex relationship between hemodynamic parameters and AD pathology. Finally, our study only examined one-time points (12 weeks), and it is possible that longer development of mice may have different effects on hemodynamic parameters and AD pathology, as the latter is linked to aging.

Methods

Animals. All animal protocols were approved by the Institutional Animal Care and Use Committee of Baylor College of Medicine in accordance with the National Institutes of Health Guide for the Care and Use of Laboratory Animals. We used 5 male and female littermate controls (CTR) and a mixture of male (n=10) and female (n=10) 5XFAD mice at 2-3 months of age. Diets of both groups of mice consisted of standard commercial chow (2920X Harlan Teklad, Indianapolis, IN, USA) with free access to food and water. 2.5% isoflurane initially was used for anesthesia and mice were transferred to a heated (37±1°C) electrocardiography board

(MouseMonitor S, Indus Instruments, Webster, TX) with isoflurane maintained at 1.5%. Electrodes on mice paws were utilized to measure electrocardiogram (ECG).

Doppler flow velocity measurements. 10 MHz Doppler probe was used to measure doppler aortic outflow velocity and mitral inflow signals. As per previous reports (Marshall et al., 2022), using Doppler Flow Velocity System (DFVS; Indus Instruments, Webster, TX), all signals (including blood pressure and ECG) were simultaneously acquired. Peak (Vp) and mean (Vm) aortic velocities, stroke distance (Sd), ejection time (ET), peak (Ap) and mean (Am) aortic accelerations, Mitral early peak € and atrial peak (A) velocities, E/A ratio, deceleration time (DT) isovolumic contraction (IVCT) & relaxation (IVRT) times, and myocardial performance index (M–I – also known as Tei index), were able to be determined from cardiac Doppler signals.

Blood pressure and flow velocity measurements. As previously described (Reddy et al., 2005; Hinton Jr et al., 2016; Marshall et al., 2022), blood pressure was measured. The right carotid artery was intubated with a pressure catheter (SPR-1000: Millar Instruments, Inc., Houston, TX) following isolation. The ascending aorta measured aortic pressure, while aortic pressure and velocity signals were displayed simultaneously with 2 second segments of both signals recorded using the DFVS system. The catheter was then advanced into the LV, with 2-s segments of LV pressure. Systolic blood pressure (SBP), diastolic blood pressure (DBP), mean blood pressure (MBP), pulse pressure (PP), and rate-pressure product (RPP) were calculated from aortic pressure.

Determination of aortic input impedance. Using previously published techniques (Reddy et al., 2003, 2005, 2014; Hinton Jr et al., 2016; Marshall et al., 2022), aortic and cerebral impedance was determined. The pressure and velocity waveforms were processed using discrete Fourier transform to determine aortic and cerebral input impedance (Zi). Peripheral vascular resistance (Zp – impedance at zero frequency), impedance at first harmonic (Z_1), characteristic impedance (Zc – average of 2nd to 10th harmonic) were extracted from the modulus of aortic and cereberal impedance (|Zi|). PWV was determined as |Zi| as Zc/ρ (ρ - density of blood).

Calculation of parameters to determine VVC. Arterial elastance (Ea) was calculated as ESP/SV (stroke volume, SV=Sd*aortic cross-sectional area), end systolic elastance (Ees) was calculated as ESP/ESV, ventricular-vascular coupling (VVC) was calculated as Ea/Ees, and stroke work (SW) was calculated as ESP*SV (Tona et al., 2021; Marshall et al., 2022).

Statistical analyses. All the data are presented as mean ± standard error of the mean (SEM). Dots represent each sample, as sample size varies throughout. Statistical analyses were performed via analysis using unpaired T-test or One-way ANOVA on Prism (GraphPad Software; La Jolla, USA).

Acknowledgment:

FUNDING

This work is supported by National Institute of Health (NIH) NIDDK T-32, number DK007563 entitled Multidisciplinary Training in Molecular Endocrinology to Z.V.; The United Negro College Fund/Bristol-Myers Squibb E.E. Just Faculty Fund, Burroughs Wellcome Fund Career Awards at the Scientific Interface Award, Burroughs Wellcome Fund Ad-hoc Award, National Institutes of Health Small Research Pilot Subaward to 5R25HL106365-12 from the National Institutes of Health PRIDE Program, DK020593, Vanderbilt Diabetes and Research Training Center for DRTC Alzheimer's Disease Pilot & Feasibility Program to A.H.J. Its contents are solely the responsibility of the authors and do not necessarily represent the official view of the NIH. The funders had no role in study design, data collection and analysis, decision to publish, or preparation of the manuscript.

Disclosures

Dr. Reddy is a collaborator and consultant with Indus Instruments, Webster, TX. All other authors have no competing interests.

Author Contributions

A–M - 3456, –N - 3456, –V - 3456, H–B - 34, –G - 34, –V - 34, –B - 34, –E - 34, –A - 34, AM – 34, ES-34, AC-34, JD -34, DS – 34, SD – 34, T–P - 23, J–G - 678, –E - 678, –D - 678, M–E - 7,8, G–T - 5678, A–H - 5678, A–R - 12345678

1 Conceived and designed research, 2 Performed experiments and Data collection, 3 Data analysis, 4 Prepared figures, 5 Interpretation of results, 6 Drafted manuscript, 7 Edited and revised manuscript, 8 Approved final version of manuscript.

References

Alhakak, A. S., Møgelvang, R., Schnohr, P., Modin, D., Brainin, P., Gislason, G., et al. (2020). The cardiac isovolumetric contraction time is an independent predictor of incident heart failure in the general population. *Int J Cardiol* 312, 81–86. doi: 10.1016/j.ijcard.2020.03.046.

Alhakak, A. S., Teerlink, J. R., Lindenfeld, J., Böhm, M., Rosano, G. M. C., and Biering-Sørensen, T. (2021). The significance of left ventricular ejection time in heart failure with reduced ejection fraction. *Eur J Heart Fail* 23, 541–551. doi: 10.1002/ejhf.2125.

Bajwa, E., and Klegeris, A. (2022). Neuroinflammation as a mechanism linking hypertension with the increased risk of Alzheimer's disease. *Neural Regen Res* 17, 2342–2346. doi: 10.4103/1673-5374.336869.

Belohlavek, M., Jiamsripong, P., Calleja, A. M., McMahon, E. M., Maarouf, C. L., Kokjohn, T. A., et al. (2009). Patients With Alzheimer Disease Have Altered Transmitral Flow. *Journal of Ultrasound in Medicine* 28, 1493–1500. doi: 10.7863/jum.2009.28.11.1493.

Bink, D. I., Ritz, K., Aronica, E., Van Der Weerd, L., and Daemen, M. J. (2013). Mouse models to study the effect of cardiovascular risk factors on brain structure and cognition. *Journal of Cerebral Blood Flow & Metabolism* 33, 1666–1684.

Bugrova, A. E., Strelnikova, P. A., Indeykina, M. I., Kononikhin, A. S., Zakharova, N. V., Brzhozovskiy, A. G., et al. (2022). The Dynamics of β-Amyloid Proteoforms Accumulation in the Brain of a 5xFAD Mouse Model of Alzheimer's Disease. *International Journal of Molecular Sciences* 23, 27. doi: 10.3390/ijms23010027.

Burke, G. L., and Hughes, T. M. (2021). Arterial Changes Connecting Hypertension to Alzheimer's Disease and Related Dementias∗. *JACC: Cardiovascular Imaging* 14, 186–188. doi: 10.1016/j.jcmg.2020.10.018.

Çalık, A. N., Özcan, K. S., Yüksel, G., Güngör, B., Aruğarslan, E., Varlibas, F., et al. (2014). Altered diastolic function and aortic stiffness in Alzheimer's disease. *Clinical Interventions in Aging* 9, 1115–1121. doi: 10.2147/CIA.S63337.

Carluccio, E., Biagioli, P., Alunni, G., Murrone, A., Zuchi, C., Biscottini, E., et al. (2012). Improvement of Myocardial Performance (Tei) Index Closely Reflects Intrinsic Improvement of Cardiac Function: Assessment in Revascularized Hibernating Myocardium. *Echocardiography* 29, 298–306. doi: 10.1111/j.1540-8175.2011.01575.x.

Cho, E. J., Caracciolo, G., Khandheria, B. K., Steidley, D. E., Scott, R., Abhayaratna, W. P., et al. (2010). Tissue Doppler Image-Derived Measurements During Isovolumic Contraction Predict Exercise Capacity in Patients With Reduced Left Ventricular Ejection Fraction. *JACC: Cardiovascular Imaging* 3, 1–9. doi: 10.1016/j.jcmg.2009.08.011.

Dambrauskaite, V., Delcroix, M., Claus, P., Herbots, L., Palecek, T., D'hooge, J., et al. (2005). The Evaluation of Pulmonary Hypertension Using Right Ventricular Myocardial Isovolumic Relaxation Time. *Journal of the American Society of Echocardiography* 18, 1113–1120. doi: 10.1016/j.echo.2005.07.019.

de la Torre, J. C. (2016). Cerebral Perfusion Enhancing Interventions: A New Strategy for the Prevention of Alzheimer Dementia. *Brain Pathology* 26, 618–631. doi: 10.1111/bpa.12405.

DeBay, D. R., Phi, T.-T., Bowen, C. V., Burrell, S. C., and Darvesh, S. (2022). No difference in cerebral perfusion between the wild-type and the 5XFAD mouse model of Alzheimer's disease. *Sci Rep* 12, 22174. doi: 10.1038/s41598-022-26713-x.

DeCarli, C. (2021). The link between blood pressure and Alzheimer's disease. *The Lancet Neurology* 20, 878–879. doi: 10.1016/S1474-4422(21)00340-9.

Eglit, G. M. L., Weigand, A. J., Nation, D. A., Bondi, M. W., and Bangen, K. J. (2020). Hypertension and Alzheimer's disease: indirect effects through circle of Willis atherosclerosis. *Brain Commun* 2, fcaa114. doi: 10.1093/braincomms/fcaa114.

Eimer, W. A., and Vassar, R. (2013). Neuron loss in the 5XFAD mouse model of Alzheimer's disease correlates with intraneuronal Aβ42 accumulation and Caspase-3 activation. *Molecular Neurodegeneration* 8, 2. doi: 10.1186/1750-1326-8-2.

Fleisher, A. S., Podraza, K. M., Bangen, K. J., Taylor, C., Sherzai, A., Sidhar, K., et al. (2009). Cerebral perfusion and oxygenation differences in Alzheimer's disease risk. *Neurobiology of Aging* 30, 1737–1748. doi: 10.1016/j.neurobiolaging.2008.01.012.

Heffernan, K. S., Jae, S. Y., and Loprinzi, P. D. (2020). Association Between Estimated Pulse Wave Velocity and Mortality in U.S. Adults. *Journal of the American College of Cardiology* 75, 1862–1864. doi: 10.1016/j.jacc.2020.02.035.

Henskens, L. H. G., Kroon, A. A., van Oostenbrugge, R. J., Gronenschild, E. H. B. M., Fuss-Lejeune, M. M. J. J., Hofman, P. A. M., et al. (2008). Increased Aortic Pulse Wave Velocity Is Associated With Silent Cerebral Small-Vessel Disease in Hypertensive Patients. *Hypertension* 52, 1120–1126. doi: 10.1161/HYPERTENSIONAHA.108.119024.

Hinton Jr, A. O., Yang, Y., Quick, A. P., Xu, P., Reddy, C. L., Yan, X., et al. (2016). SRC-1 Regulates Blood Pressure and Aortic Stiffness in Female Mice. *PLOS ONE* 11, e0168644. doi: 10.1371/journal.pone.0168644.

Homan, T. D., Bordes, S., and Cichowski, E. (2018). Physiology, pulse pressure.

Hughes, T. M., Craft, S., and Lopez, O. L. (2015). Review of 'the potential role of arterial stiffness in the pathogenesis of Alzheimer's disease.' *Neurodegener Dis Manag* 5, 121–135. doi: 10.2217/nmt.14.53.

Hughes, T. M., Kuller, L. H., Barinas-Mitchell, E. J. M., Mackey, R. H., McDade, E. M., Klunk, W. E., et al. (2013). Pulse wave velocity is associated with β-amyloid deposition in the brains of very elderly adults. *Neurology* 81, 1711–1718. doi: 10.1212/01.wnl.0000435301.64776.37.

Igarashi, H., Ueki, S., Kitaura, H., Kera, T., Ohno, K., Ohkubo, M., et al. (2020). Longitudinal GluCEST MRI changes and cerebral blood flow in 5xFAD mice. *Contrast Media & Molecular Imaging* 2020, 1–12.

Lennon, M. J., Makkar, S. R., Crawford, J. D., and Sachdev, P. S. (2019). Midlife Hypertension and Alzheimer's Disease: A Systematic Review and Meta-Analysis. *J Alzheimers Dis* 71, 307–316. doi: 10.3233/JAD-190474.

Liu, L., Chen, B., Zhang, X., Tan, L., and Wang, D. W. (2017). Increased Cathepsin D Correlates with Clinical Parameters in Newly Diagnosed Type 2 Diabetes. *Disease Markers* 2017, e5286408. doi: 10.1155/2017/5286408.

Marshall, A. G., Neikirk, K., Vue, Z., Beasley, H. K., Garza-Lopez, E., Vang, L., et al. (2022). Cardiovascular Hemodynamics in Mice with Tumor Necrosis Factor Receptor - Associated Factor 2 Mediated Cytoprotection in the Heart. 2022.09.03.506447. doi: 10.1101/2022.09.03.506447.

McEniery, C. M., Yasmin, Hall, I. R., Qasem, A., Wilkinson, I. B., and Cockcroft, J. R. (2005). Normal Vascular Aging: Differential Effects on Wave Reflection and Aortic Pulse Wave

Velocity: The Anglo-Cardiff Collaborative Trial (ACCT). *Journal of the American College of Cardiology* 46, 1753–1760. doi: 10.1016/j.jacc.2005.07.037.

Nilsson, E. D., Elmståhl, S., Minthon, L., Pihlsgård, M., Nilsson, P. M., Hansson, O., et al. (2017). No independent association between pulse wave velocity and dementia: a population-based, prospective study. *Journal of Hypertension* 35, 2462–2467. doi: 10.1097/HJH.0000000000001480.

Oakley, H., Cole, S. L., Logan, S., Maus, E., Shao, P., Craft, J., et al. (2006). Intraneuronal beta-amyloid aggregates, neurodegeneration, and neuron loss in transgenic mice with five familial Alzheimer's disease mutations: potential factors in amyloid plaque formation. *J Neurosci* 26, 10129–10140. doi: 10.1523/JNEUROSCI.1202-06.2006.

Obata, Y., Mizogami, M., Singh, S., Nyhan, D., Berkowitz, D. E., Steppan, J., et al. (2017). Ejection time: influence of hemodynamics and site of measurement in the arterial tree. *Hypertens Res* 40, 811–818. doi: 10.1038/hr.2017.43.

Oblak, A. L., Lin, P. B., Kotredes, K. P., Pandey, R. S., Garceau, D., Williams, H. M., et al. (2021). Comprehensive Evaluation of the 5XFAD Mouse Model for Preclinical Testing Applications: A MODEL-AD Study. *Frontiers in Aging Neuroscience* 13. Available at: https://www.frontiersin.org/articles/10.3389/fnagi.2021.713726 [Accessed March 28, 2023].

Palta, P., Sharrett, A. R., Wei, J., Meyer, M. L., Kucharska□Newton, A., Power, M. C., et al. (2019). Central Arterial Stiffness Is Associated With Structural Brain Damage and Poorer Cognitive Performance: The ARIC Study. *Journal of the American Heart Association* 8, e011045. doi: 10.1161/JAHA.118.011045.

Pase, M. P., Beiser, A., Himali, J. J., Tsao, C., Satizabal, C. L., Vasan, R. S., et al. (2016). Aortic Stiffness and the Risk of Incident Mild Cognitive Impairment and Dementia. *Stroke* 47, 2256–2261. doi: 10.1161/STROKEAHA.116.013508.

Rabkin, S. W., and Jarvie, G. (2011). Comparison of vascular stiffness in vascular dementia, Alzheimer dementia and cognitive impairment. *Blood Pressure* 20, 274–283. doi: 10.3109/08037051.2011.566246.

Reddy, A. K., Hartley, C. J., Pham, T. T., Darlington, G., Entman, M. L., and Taffet, G. E. (2014). Young Little Mice Express a Premature Cardiovascular Aging Phenotype. *The Journals of Gerontology: Series A* 69A, 152–159. doi: 10.1093/gerona/glt055.

Reddy, A. K., Li, Y.-H., Pham, T. T., Ochoa, L. N., Treviño, M. T., Hartley, C. J., et al. (2003). Measurement of aortic input impedance in mice: effects of age on aortic stiffness. *American Journal of Physiology-Heart and Circulatory Physiology* 285, H1464–H1470. doi: 10.1152/ajpheart.00004.2003.

Reddy, A. K., Taffet, G. E., Li, Y.-H., Lim, S.-W., Pham, T. T., Pocius, J. S., et al. (2005). Pulsed Doppler signal processing for use in mice: applications. *IEEE Transactions on Biomedical Engineering* 52, 1771–1783. doi: 10.1109/TBME.2005.855709.

Ren, D., Fu, Y., Wang, L., Liu, J., Zhong, X., Yuan, J., et al. (2021). Tetrandrine ameliorated Alzheimer's disease through suppressing microglial inflammatory activation and neurotoxicity in the 5XFAD mouse. *Phytomedicine* 90, 153627. doi: 10.1016/j.phymed.2021.153627.

Rivera-Rivera, L. A., Cody, K. A., Eisenmenger, L., Cary, P., Rowley, H. A., Carlsson, C. M., et al. (2021). Assessment of vascular stiffness in the internal carotid artery proximal to the carotid canal in Alzheimer's disease using pulse wave velocity from low rank reconstructed 4D flow MRI. *Journal of Cerebral Blood Flow & Metabolism* 41, 298–311.

Roher, A. E., Debbins, J. P., Malek-Ahmadi, M., Chen, K., Pipe, J. G., Maze, S., et al. (2012). Cerebral blood flow in Alzheimer's disease. *Vascular Health and Risk Management* 8, 599–611. doi: 10.2147/VHRM.S34874.

Scheltens, P., Blennow, K., Breteler, M. M. B., de Strooper, B., Frisoni, G. B., Salloway, S., et al. (2016). Alzheimer's disease. *The Lancet* 388, 505–517. doi: 10.1016/S0140-6736(15)01124-1.

Shih, Y.-H., Wu, S.-Y., Yu, M., Huang, S.-H., Lee, C.-W., Jiang, M.-J., et al. (2018). Hypertension Accelerates Alzheimer's Disease-Related Pathologies in Pigs and 3xTg Mice. *Frontiers in Aging Neuroscience* 10. Available at: https://www.frontiersin.org/articles/10.3389/fnagi.2018.00073 [Accessed June 8, 2023].

Silva, M. V. F., Loures, C. de M. G., Alves, L. C. V., de Souza, L. C., Borges, K. B. G., and Carvalho, M. das G. (2019). Alzheimer's disease: risk factors and potentially protective measures. *J Biomed Sci* 26, 33. doi: 10.1186/s12929-019-0524-y.

Tarumi, T., and Zhang, R. (2014). Cerebral hemodynamics of the aging brain: risk of Alzheimer disease and benefit of aerobic exercise. *Frontiers in Physiology* 5. Available at: https://www.frontiersin.org/articles/10.3389/fphys.2014.00006 [Accessed June 8, 2023].

Tona, F., Zanatta, E., Montisci, R., Muraru, D., Beccegato, E., De Zorzi, E., et al. (2021). Higher Ventricular-Arterial Coupling Derived from Three-Dimensional Echocardiography Is Associated with a Worse Clinical Outcome in Systemic Sclerosis. *Pharmaceuticals (Basel)* 14, 646. doi: 10.3390/ph14070646.

Waldstein, S. R., Rice, S. C., Thayer, J. F., Najjar, S. S., Scuteri, A., and Zonderman, A. B. (2008). Pulse pressure and pulse wave velocity are related to cognitive decline in the Baltimore Longitudinal Study of Aging. *Hypertension* 51, 99–104. doi: 10.1161/HYPERTENSIONAHA.107.093674.

Wong, W. (2020). Economic burden of Alzheimer disease and managed care considerations. *Am J Manag Care* 26, S177–S183. doi: 10.37765/ajmc.2020.88482.

Zeng, X., Fu, X., Li, X., Zhou, J., Huang, S., Li, X., et al. (2019). Association Between Carotid-Cerebral Pulse Wave Velocity and Acute Ischemic Stroke: Clinical Trial Protocol.

Journal of Stroke and Cerebrovascular Diseases 28, 2580–2584. doi: 10.1016/j.jstrokecerebrovasdis.2019.03.045.

Zhang, L., Zhang, S., Maezawa, I., Trushin, S., Minhas, P., Pinto, M., et al. (2015). Modulation of Mitochondrial Complex I Activity Averts Cognitive Decline in Multiple Animal Models of Familial Alzheimer's Disease. *EBioMedicine* 2, 294–305. doi: 10.1016/j.ebiom.2015.03.009.

Figure Legend:

Figure 1: General parameters and velocity parameters of male and female control and 5XFAD mice. (**A**) Body weight in grams, (**B**) aortic cross-sectional area, and (**C**) heart rate (HR) in beats per minute are shown. (**D**) Peak aortic outflow velocity (**E**) mean outflow velocity, and (**F**) aortic ejection time. Data are presented as mean±SEM (n = 5-10/group). * represents $p < 0.05$, ns indicates a statistically non-significant relationship.

Figure 2: Carotid velocity parameters of male and female control and 5XFAD mice. (**A**) Peak carotid outflow velocity, (**B**) minimum carotid outflow velocity, (**C**) mean carotid outflow, (**D**) pulsatility index (PI), a measure of resistance calculated by (V_{max} - V_{min}) / Mean velocity. (**E**) resistivity index (RI), a measure of resistance to blood flow calculated by (V_{max} - V_{min}) / V_{max}. Data are presented as mean±SEM (n = 5-10/group). * represents $p < 0.05$, ns indicates a statistically non-significant relationship.

Figure 3: Blood pressure parameters of male and female control and 5XFAD mice. (**A)** Systolic blood pressure (SBP), (**B**) Diastolic blood pressure (DBP), (**C**) Mean blood pressure (MBP), (**D**) Pulse pressure, and (**E**) Rate pressure product. Data are presented as mean±SEM (n = 5-10/group). *, ** represents $p < 0.05$, $p < 0.01$, respectively, and ns indicates a statistically non-significant relationship.

Figure 4: Parameters of aortic impedance in male and female 5XFAD and stressed-5XFAD mice. (**A**) Total peripheral resistance (Z_P), (**B**) impedance at first harmonic (Z_1), (**C**) characteristic impedance, (Z_C) (**D**), and impedance-based pulse wave velocity (PWV). Data are presented as mean±SEM (n = 5-10/group). *, ** represents $p < 0.05$, $p < 0.01$, respectively, and ns indicates a statistically non-significant relationship.

Figure 5: Parameters of cereberal impedance in male and female 5XFAD and stressed-5XFAD mice. (**A**) Total cerebral peripheral resistance (Z_P), (**B**) impedance at first harmonic (Z_1), (**C**) characteristic impedance, (Z_C) (**D**), and impedance-based pulse wave velocity (PWV). Data are presented as mean±SEM (n = 5-10/group). *, ** represents $p < 0.05$, $p < 0.01$, respectively, and ns indicates a statistically non-significant relationship.

Figure 6: Mitral flow velocity parameters of male and female chow diet 5XFAD mice and control littermates. (**A**) end systolic pressure, (**B**) aortic elastance, (**C**) stroke work, (**D**) stroke distance. Data are presented as mean±SEM (n = 5-10/group). *, ** represents $p < 0.05$, $p < 0.01$, respectively, and ns indicates a statistically non-significant relationship.

Figure 7: Ventricular-vascular coupling indices parameters of male and female chow diet 5XFAD mice and control littermates (**A**) peak mitral-early flow velocity, (**B**) isovolumic relaxation time, (**C**) isovolumic contraction time, (**D**) myocardial performance index (Tei index). Data are presented as mean±SEM (n = 5-10/group). *, ** represents $p < 0.05$, $p < 0.01$, respectively, and ns indicates a statistically non-significant relationship.

Supplemental Figures:

Table 1: Summary of Pulse Wave, Doppler Ultrasound, Aortic and Cerebral Impedance Measurements Utilized.

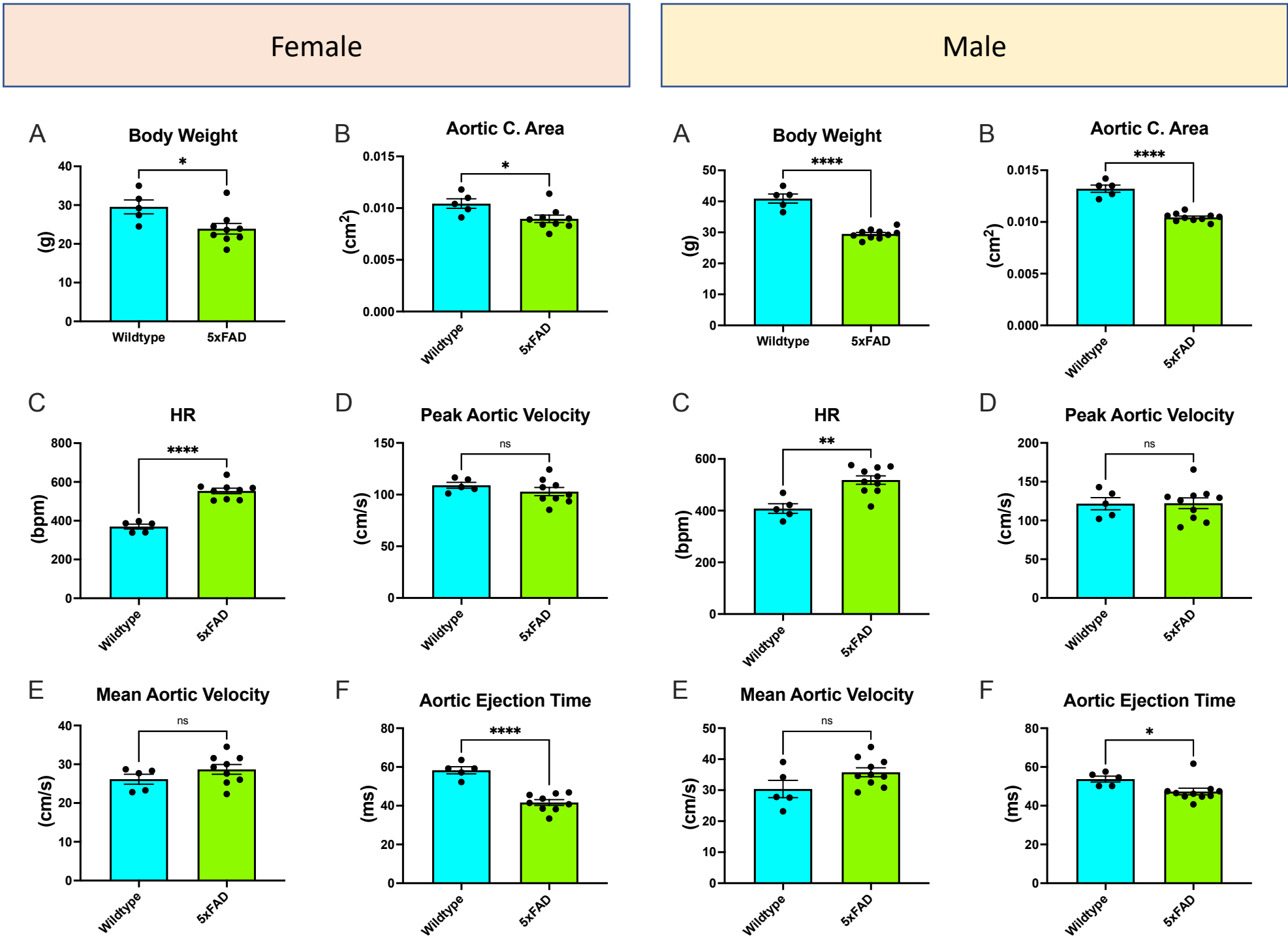
Female
Male
A
Body Weight
(g)
Wildtype
5xFAD
B
Aortic C. Area
(cm2)
C
HR
(bpm)
D
Peak Aortic Velocity
(cm/s)
ns
E
Mean Aortic Velocity
(cm/s)
F
Aortic Ejection Time
(ms)
*
**
****

Female

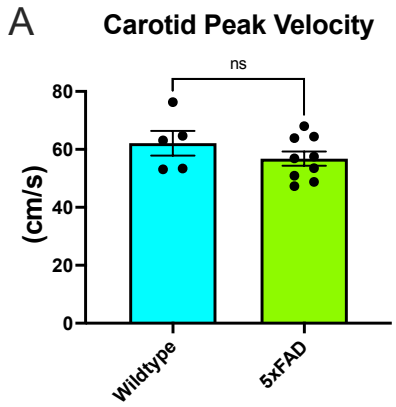
A
Carotid Peak Velocity
ns
(cm/s)
80
60
40
20
0
Wildtype
5xFAD

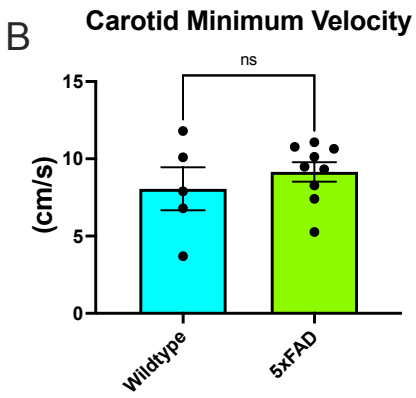
B
Carotid Minimum Velocity
ns
(cm/s)
15
10
5
0
Wildtype
5xFAD

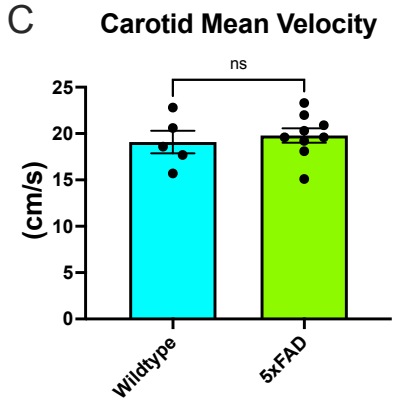
C
Carotid Mean Velocity
ns
(cm/s)
25
20
15
10
5
0
Wildtype
5xFAD

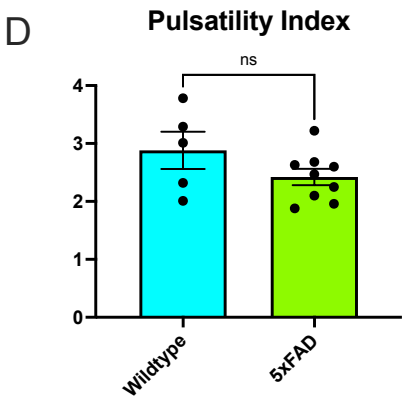
D
Pulsatility Index
ns
4
3
2
1
0
Wildtype
5xFAD

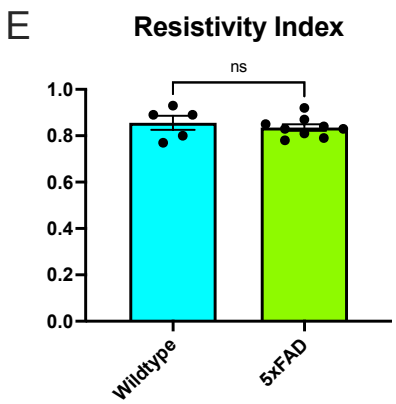
E
Resistivity Index
ns
1.0
0.8
0.6
0.4
0.2
0.0
Wildtype
5xFAD

Male

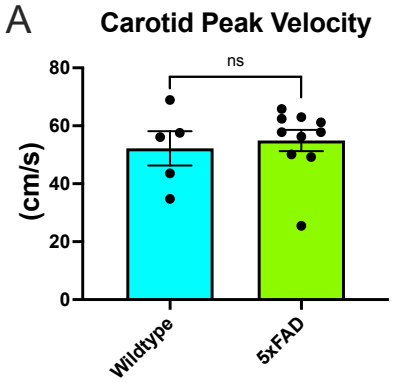
A
Carotid Peak Velocity
ns
(cm/s)
80
60
40
20
0
Wildtype
5xFAD

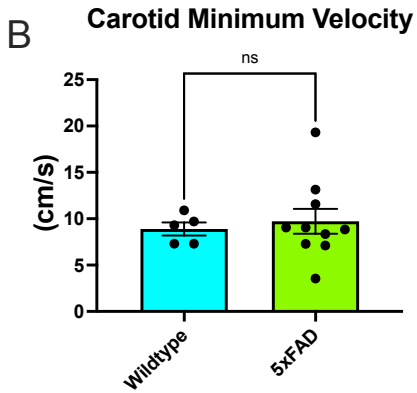
B
Carotid Minimum Velocity
ns
(cm/s)
25
20
15
10
5
0
Wildtype
5xFAD

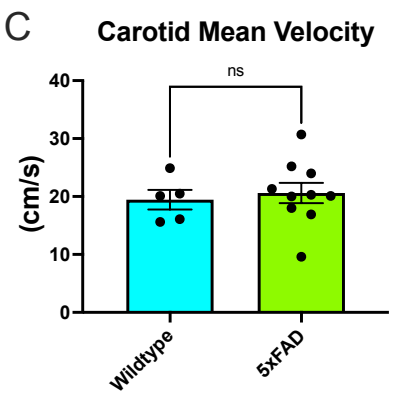
C
Carotid Mean Velocity
ns
(cm/s)
40
30
20
10
0
Wildtype
5xFAD

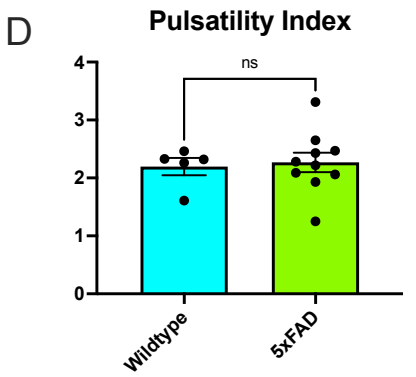
D
Pulsatility Index
ns
4
3
2
1
0
Wildtype
5xFAD

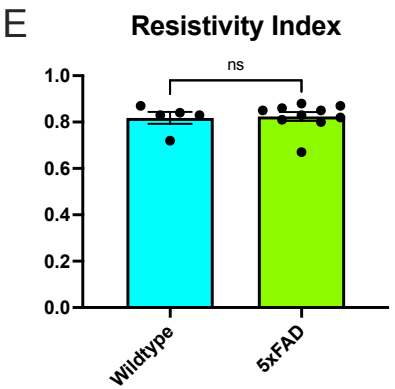
E
Resistivity Index
ns
1.0
0.8
0.6
0.4
0.2
0.0
Wildtype
5xFAD

Female

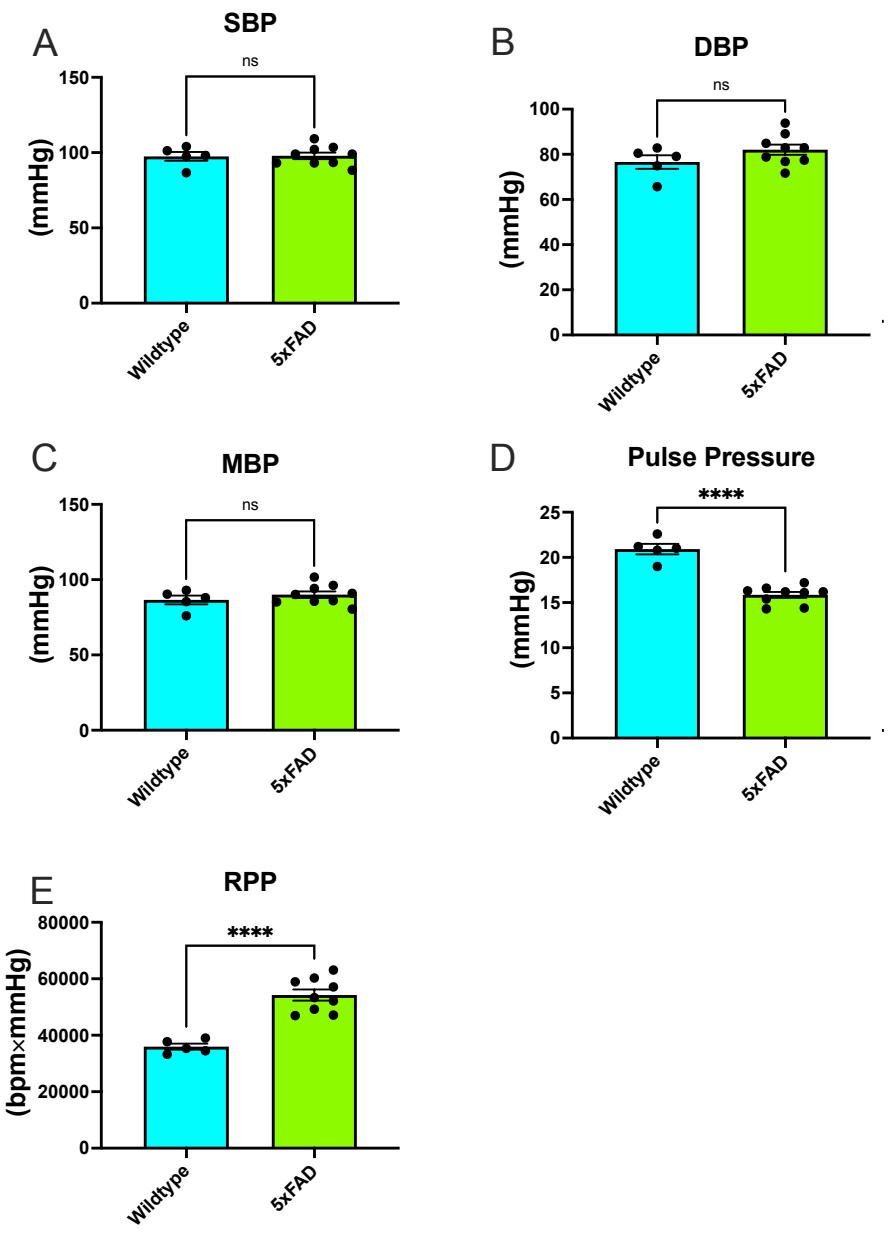
A
SBP
ns
(mmHg)
150
100
50
0
Wildtype
5xFAD
B
DBP
ns
(mmHg)
100
80
60
40
20
0
Wildtype
5xFAD
C
MBP
ns
(mmHg)
150
100
50
0
Wildtype
5xFAD
D
Pulse Pressure
****
(mmHg)
25
20
15
10
5
0
Wildtype
5xFAD
E
RPP
****
(bpm×mmHg)
80000
60000
40000
20000
0
Wildtype
5xFAD

Male

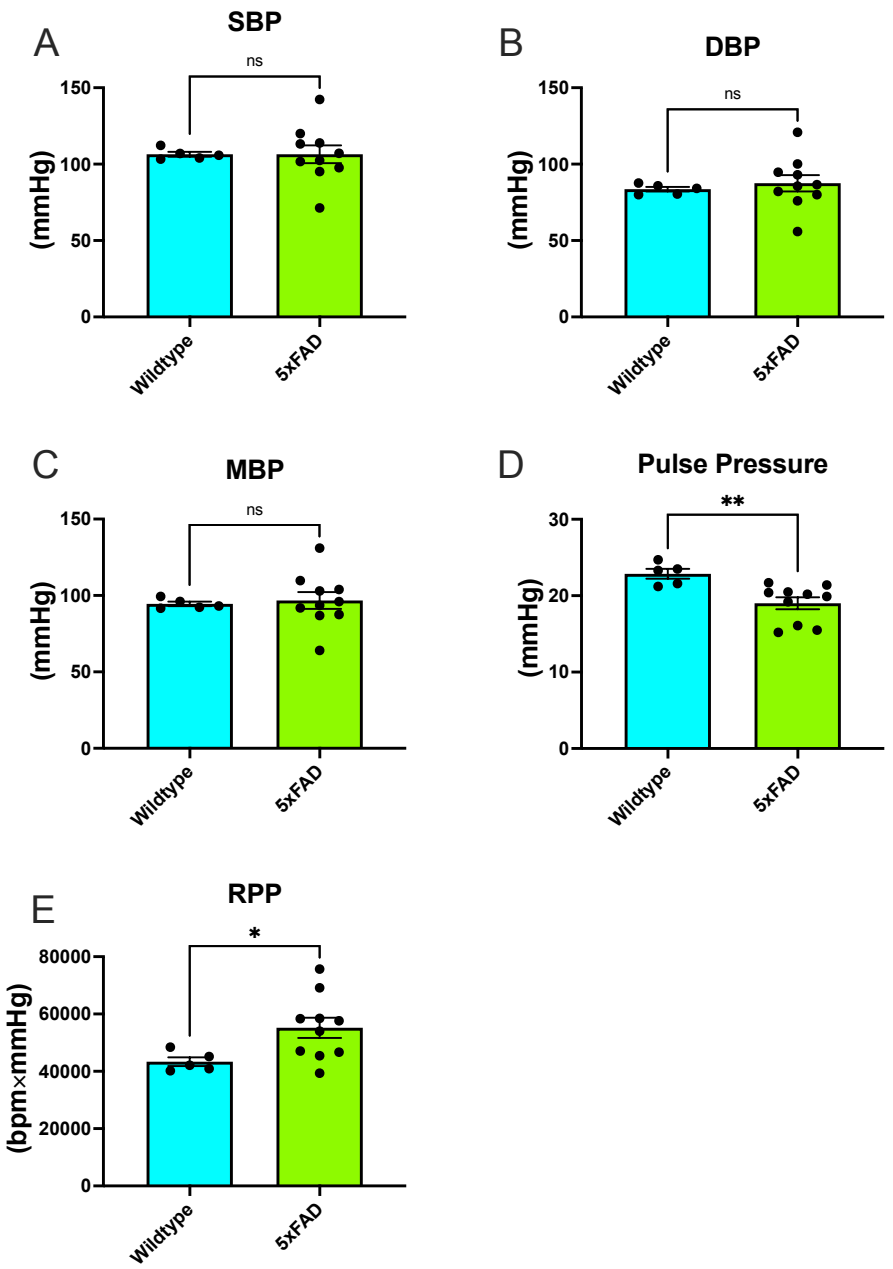
A
SBP
ns
(mmHg)
150
100
50
0
Wildtype
5xFAD
B
DBP
ns
(mmHg)
150
100
50
0
Wildtype
5xFAD
C
MBP
ns
(mmHg)
150
100
50
0
Wildtype
5xFAD
D
Pulse Pressure
**
(mmHg)
30
20
10
0
Wildtype
5xFAD
E
RPP
*
(bpm×mmHg)
80000
60000
40000
20000
0
Wildtype
5xFAD

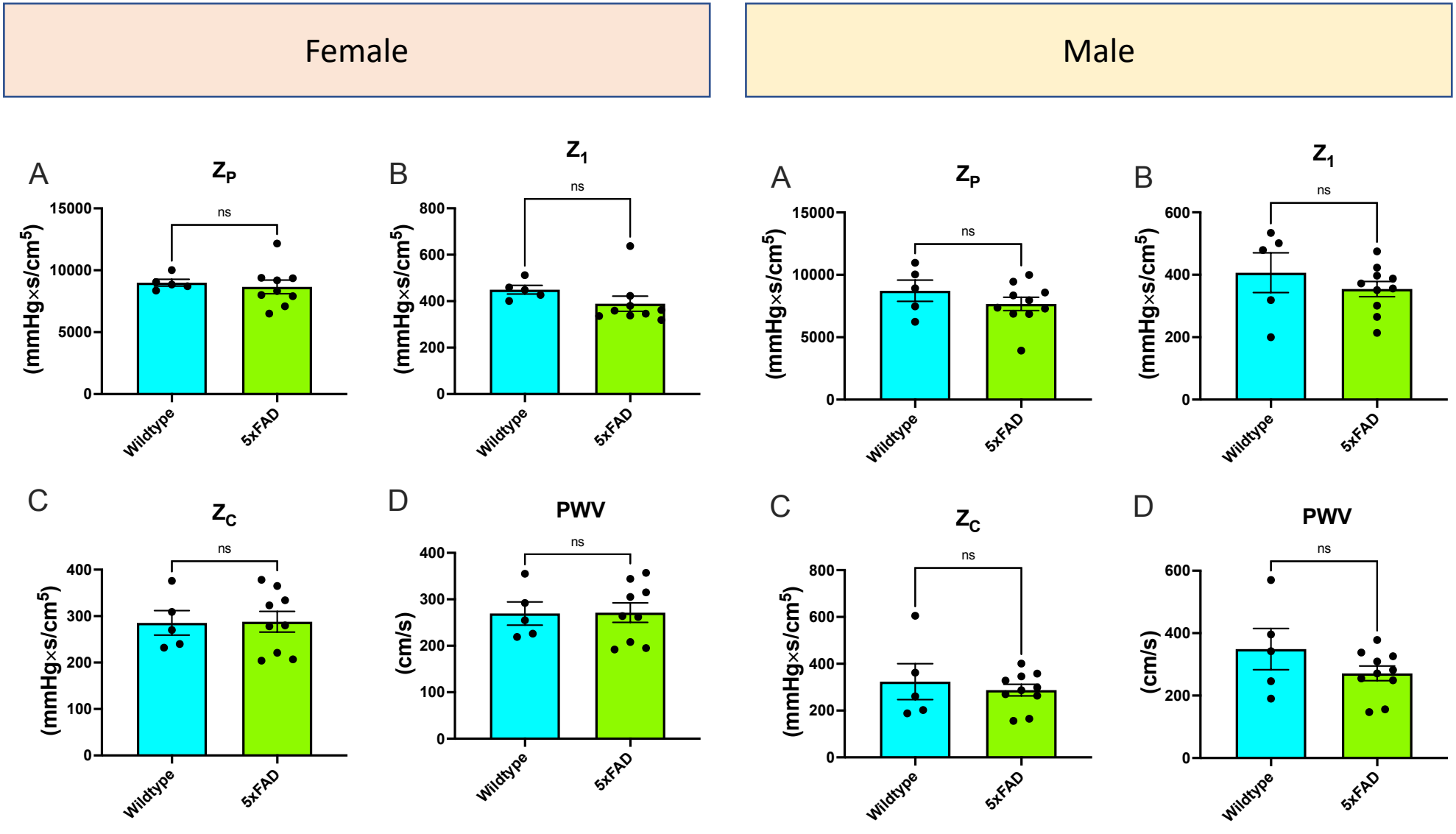
Female
Male
A
Z_P
B
Z_1
C
Z_C
D
PWV
ns
(mmHg×s/cm^5)
(cm/s)
Wildtype
5xFAD

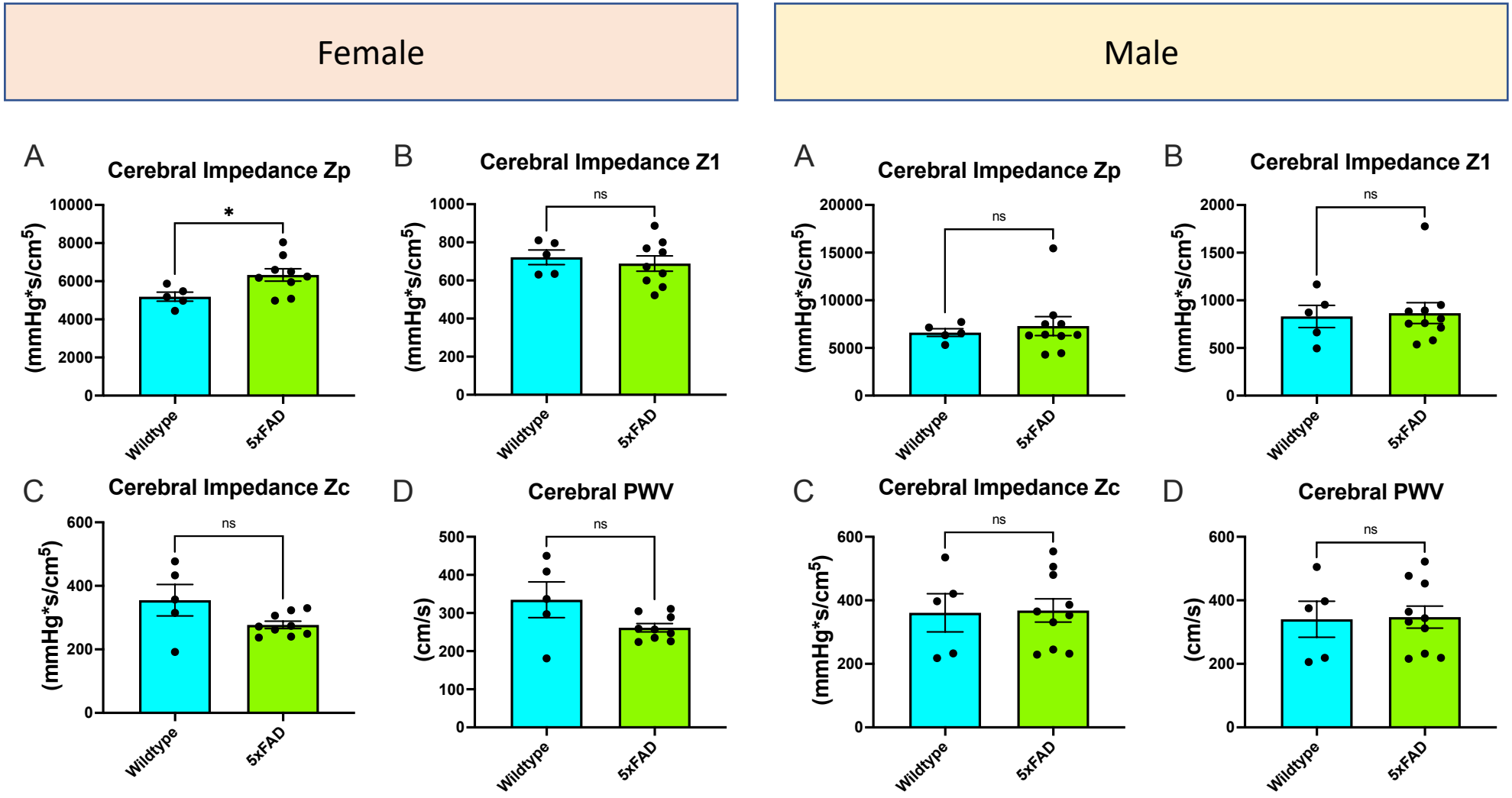
Female
Male
A
Cerebral Impedance Zp
(mmHg*s/cm5)
10000
8000
6000
4000
2000
0
*
Wildtype
5xFAD
B
Cerebral Impedance Z1
(mmHg*s/cm5)
1000
800
600
400
200
0
ns
Wildtype
5xFAD
C
Cerebral Impedance Zc
(mmHg*s/cm5)
600
400
200
0
ns
Wildtype
5xFAD
D
Cerebral PWV
(cm/s)
500
400
300
200
100
0
ns
Wildtype
5xFAD
A
Cerebral Impedance Zp
(mmHg*s/cm5)
20000
15000
10000
5000
0
ns
Wildtype
5xFAD
B
Cerebral Impedance Z1
(mmHg*s/cm5)
2000
1500
1000
500
0
ns
Wildtype
5xFAD
C
Cerebral Impedance Zc
(mmHg*s/cm5)
600
400
200
0
ns
Wildtype
5xFAD
D
Cerebral PWV
(cm/s)
600
400
200
0
ns
Wildtype
5xFAD

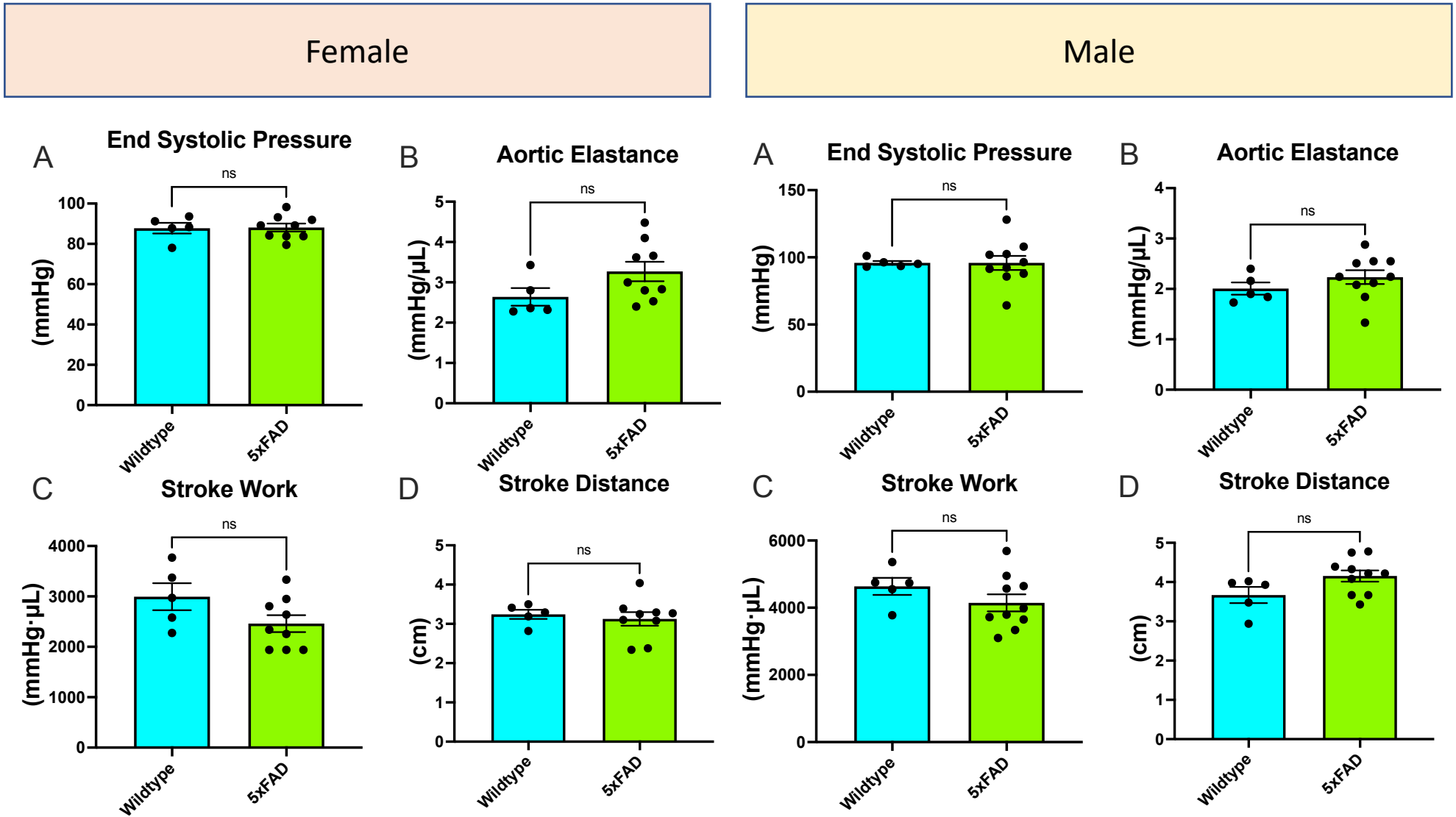
Female
Male
A
End Systolic Pressure
(mmHg)
ns
Wildtype
5xFAD
B
Aortic Elastance
(mmHg/µL)
C
Stroke Work
(mmHg·µL)
D
Stroke Distance
(cm)

Female

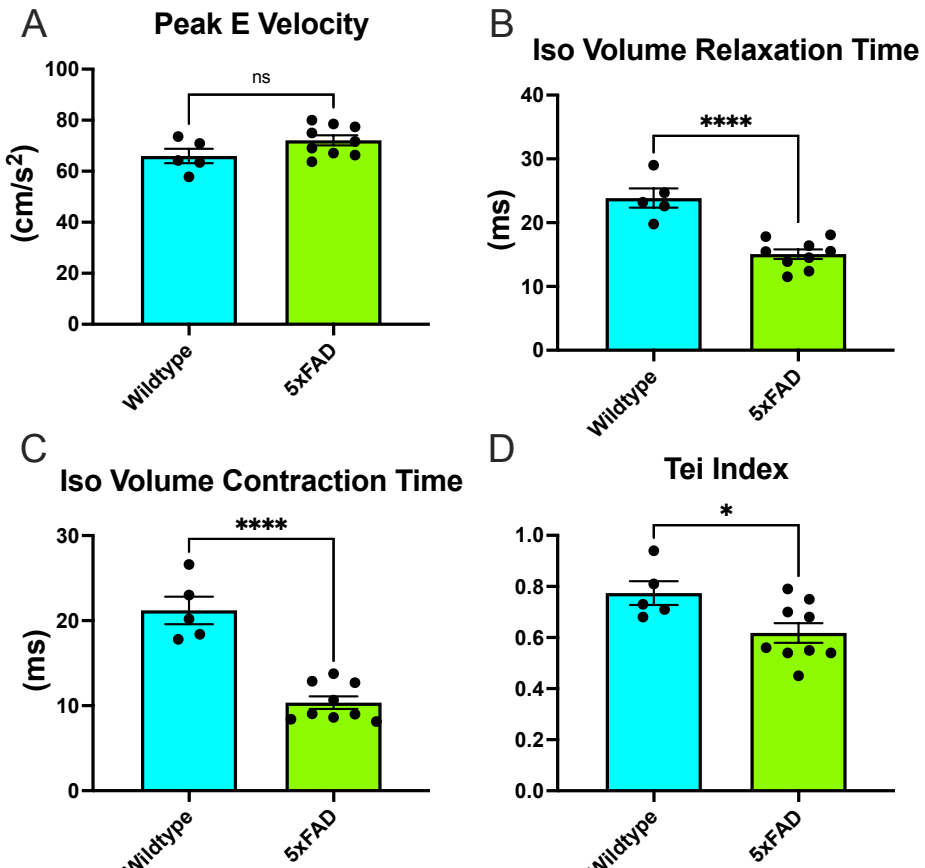
A
Peak E Velocity
(cm/s2)
ns
Wildtype
5xFAD
B
Iso Volume Relaxation Time
(ms)
****
Wildtype
5xFAD
C
Iso Volume Contraction Time
(ms)
****
Wildtype
5xFAD
D
Tei Index
*
Wildtype
5xFAD

Male

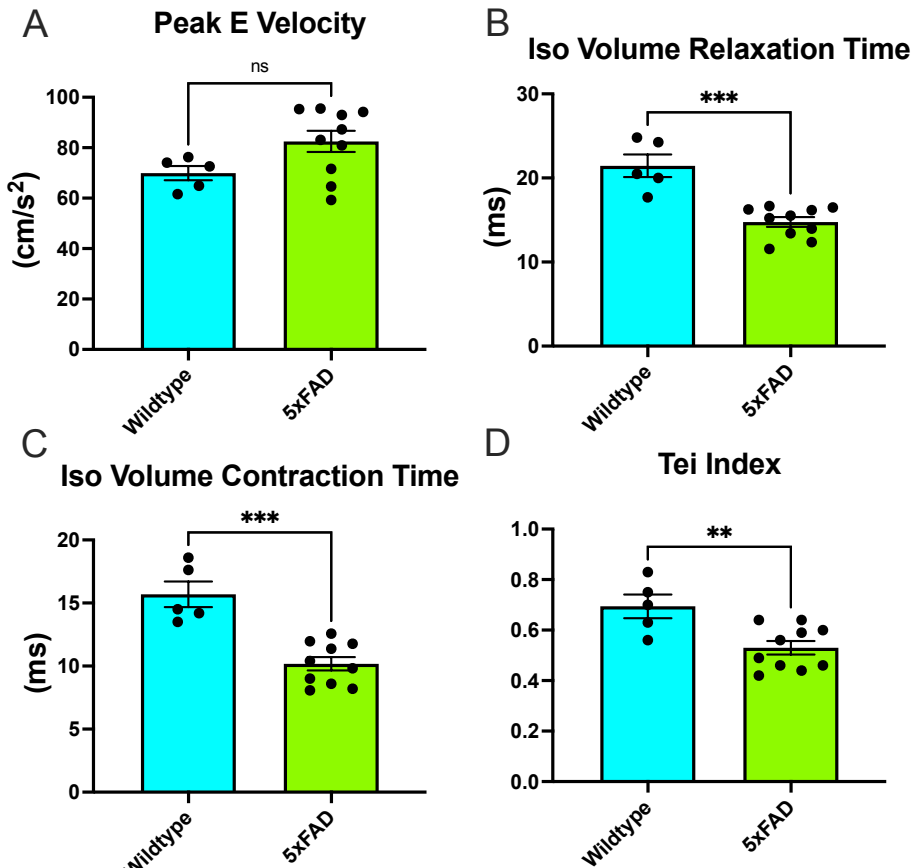
A
Peak E Velocity
(cm/s2)
ns
Wildtype
5xFAD
B
Iso Volume Relaxation Time
(ms)
***
Wildtype
5xFAD
C
Iso Volume Contraction Time
(ms)
***
Wildtype
5xFAD
D
Tei Index
**
Wildtype
5xFAD

Measurement	Definition
Aortic cross-sectional area	The area of the aorta, indicator of blood vessel size and used to calculate blood flow velocity.
Aortic ejection time	Indicator of heart function which represents time period for blood to ejected into the aorta during systole.
Aortic elastance	Stiffness of the aorta to aid in understanding vascular function.
Aortic pulse wave velocity	Velocity for pressure waves to travel through the aorta; indicator of impedance of blood flow in the arterial system.
Body weight	The overall mass of mice, as measured in grams.
Cerebral pulse wave velocity	Velocity for pressure waves to travel through the cerebral arteries, indicator of impedance of blood flow in the brain.
Cerebral Z1	Resistance to blood flow at the frequency of the first harmonic in the cerebral circulation, which is an indicator of cerebral arterial stiffness.
Cerebral ZC	The characteristic impedance of the cerebral pulse wave propagation with reflection, reflects the properties of the cerebral arteries.
Cerebral ZP	Measure of the resistance to blood flow in the cerebral circulation which is an indicator of the state of the cerebral vasculature.
Deceleration time	Time for the mitral valve to close following diastole.
End systolic pressure	Pressure in the heart at the end of systolic period used to assess cardiac output.
Heart rate (HR)	Beats per minute (bpm) general characteristic typically known to decrease with age and rudimentary indicator of cardiovascular health.
Impedance at first harmonic (Z1)	Blood flow resistance at the frequency of the first harmonic of the pulse wave, which is an indicator of arterial walls stiffness.
Impedance-based cerebral PWV	Speed at which the pulse wave travels through the cerebral arteries, as measurement of cerebral arterial stiffness.
Impedance-based pulse wave velocity (PWV)	Measure of the velocity of the arterial pulse wave as it travels through the arterial tree.
Isovolumic contraction time	Length of time between mitral valve closing and aortic valve opening during diastole.
Isovolumic relaxation time	Length of time between aortic valve closing and mitral valve opening during diastole.
Mean carotid outflow	Average velocity of blood flow through the carotid artery.
Mean outflow velocity	Average velocity of blood flow during systole in the aorta.
Minimum carotid outflow velocity	The minimum velocity of blood flow through the carotid artery during diastole.
Myocardial performance index (Tei index)	A measure of the overall function of the heart, which takes into account systolic and diastolic function, as calculated by (IVCT+IVRT)/ET.
Peak aortic outflow velocity	Maximum velocity of blood flow during systole in the aorta.
Peak carotid outflow velocity	Maximum velocity of blood flow in the carotid artery during systole.
Peak mitral-early flow velocity	Maximum velocity of blood flow in early diastole.
Pulsatility index (PI)	Also known as the Gosling index, calculated by (Vmax - Vmin) / Mean velocity, and indicator of vascular resistance.
Resistivity index (RI)	Also known as the Pourcelot indexm, resistance to blood flow calculated by (Vmax - Vmin) / Vmax which serves as an indicator of vascular resistance.
Stroke distance	The distance the average blood cell travels during systole, which is an indicator of the heart's function.
Stroke work	Also known as cardiac work, stroke volume multiplied by mean aortic pressure, which assesses the amount of work done by the heart to eject blood during systole.
Total peripheral resistance (ZP)	Resistance to blood flow in the systemic circulation, as measured by combined effects of factors including blood vessel diameter and blood viscosity. Indicator of overall cardiovascular health.
Systolic Blood Pressure	Blood pressure during beats, in the systolic phase, key measurement for factors including hypertension.
Diastolic Blood Pressure	Blood pressure in between beats, in the diastolic phase, key measurement for factors including hypertension.
Mean Blood Pressure	Average pressure across the total cardiac cycle, including systole and diastole phases, representative of systemic vascular resistance,
Pulse Pressure	Differences between systolic and diastolic blood pressure, representative of risk factors for cardiovascular disease.
Rate Pressure Product	Simply the pulse pressure is multiplied by the mean blood pressure.